

Laser Charging Enabled DBS Placement for Downlink Communications

Weiqi Liu, *Student member, IEEE*, Liang Zhang, *Member, IEEE*, and Nirwan Ansari, *Fellow, IEEE*

Abstract—Drone-mounted base-station (DBS) can empower 5G and beyond networks with additional flexibility and maneuverability, and laser charging can potentially extend the DBS’s flight time. We propose a laser charging enabled DBS framework in which a laser charging station on the ground constantly transmits energy to a quadrotor DBS in the air and the DBS provides communications for all users. The DBS is to be intelligently placed in the optimal location to provide service to the ground users in each time slot. We thus formulate the joint power and bandwidth assignment, LasEr Charing enAbled DBS placement (TELECAST) problem to jointly maximize the flight time and communications data rate. Since the TELECAST problem is NP-hard, we decompose it into two sub-problems: the joint power and bandwidth allocation problem (JPB) and the DBS placement problem. A recursive algorithm is employed to solve the JPB problem and a counting placement algorithm is used to tackle the DBS placement problem. The performance of our algorithm is superior to fixed placement algorithms and greedy resource allocation algorithm and lagrange resource allocation algorithm upon which the user data rate is improved by more than 6% and the total flight time is extended by 20%, as demonstrated in our simulation results.

Index Terms—Drone mounted base-station (DBS), laser charging, wireless communications, resource allocation

I. INTRODUCTION

Drone-mounted base-stations (DBSs) are drawing attention from industry and government in recent years for various applications. DBSs, which can empower 5G and beyond networks with additional flexibility, maneuverability and cost efficiency as compared to traditional base stations, can be deployed to provide communications services for temporary use cases in specific areas such as disaster areas and hot spots [1].

High maneuverability enables the DBS to fly to a location where it may have a high probability of line of sight (LoS) connection to ground users, thus providing a good channel condition. However, the limited battery power of a drone limits its service capabilities. The weight of a general portable base station carried by a drone varies from 1lb (0.45kg) to 2.35lb (1.07kg) [2]. For heavy lift drones, the ‘Tarot T-18 Ready To Fly’ drone with the maximum payload of 8kg has 20 minutes of flight time, ‘DJI MATRICE 600’ with the maximum payload of 6kg has 16 minutes of flight time and ‘AZ 4K UHD Camera Drone Green Bee 1200’ with 20kg

This work was supported in part by National Science Foundation under Grant CNS-1814748.

Weiqi Liu, Liang Zhang and Nirwan Ansari are with the Advanced Networking Laboratory, Department of Electrical and Computing Engineering, New Jersey Institute of Technology, Newark, NJ 07102 USA (email: wl296@njit.edu; lz284@njit.edu; nirwan.ansari@njit.edu).

payload has 20 minutes of flight time [3]. The heavy payload and limited battery capacity curtail the drone’s service range and serving time. One solution to overcome this issue is to charge the drone via wire while it is flying. For example, the 2017 hurricane Maria destroyed 90 percent of the cell sites [4] in Puerto Rico and AT&T deployed DBSs charged via wire to provide emergency cellular network service for victims [5]. However, the wire limits the range of activities of the DBS and reduces the maneuverability of the DBS; a long cable also increases the cost of deploying a DBS. As compared to the wired charging, wireless charging, e.g., via RF and laser charging, is an attractive alternative solution. Note that RF charging has a large divergence angle to charge multiple devices and it can only work in a very short distance. The laser can travel 50km in clear weather, 1.9km in fog and 500m in moderate fog [6]. Encouraged by the laser’s high energy transmission efficiency, small divergence angle and long transmission distance, the laser charging is becoming a viable solution to charge the DBS. In a millimeter-wave communication system, non-LoS links will greatly degrade the communication rate, and the deployment of DBSs will greatly increase the probability of LoS to improve the system throughput. Furthermore, the field tests illustrated by [34] and [35] have demonstrated the feasibility of charging DBSs by laser beams.

Many works on DBS communications and wireless charging of drones have been reported. Ansari *et al.* [7] first postulated the concept of enabling DBSs to simultaneously receive data and energy via the laser beams. Al-Hourani *et al.* [8] elucidated a path loss model for drone-to-ground user communications, and constructed a model to calculate the optimal altitude for a DBS to obtain the maximum coverage for a given path loss. Wang *et al.* [9] proposed to use unsupervised learning and 3D wireless channel rapid modeling to estimate the wireless channel. Zhang and Ansari [10] proposed an approximation algorithm to solve the in-band full duplex communications and 3D DBS placement problem. Mostafa *et al.* [11] built a system for a DBS to harvest energy wirelessly. Wu *et al.* [12] maximized the minimum average rate among all users by jointly optimizing the user communication scheduling and UAV trajectory. Ouyang *et al.* [13] studied a laser-powered UAV focusing on the downlink communications from the UAV to the ground base station. Jiang *et al.* [14] proposed to use the DBS to charge the ground users through RF frequency with the target to maximize the data rate from the ground users to the DBS. Sun *et al.* [15] studied the 3D placement, power and subcarrier allocation problem in a solar powered DBS communication system. Qiao *et al.* [26] studied the trajectory

of the DBS in the post-disaster area and implemented a genetic algorithm to find the best DBS trajectory to provide emergency communications for the victims. Sun *et al.* [27] studied the DBS assisted mobile access network, and they proposed a spectrum efficiency aware DBS placement and user association algorithm to obtain the optimal 3D placement and the maximum throughput of the network. Zhang *et al.* [30] developed a non-convex mathematical model for Hierarchical Heterogeneous Wireless Networks (HHWNs) and proposed control and resource allocation algorithms for HHWNS to adapt the dynamic scenarios. Hu *et al.* [31] investigated the trajectory design for a group of DBSs in dynamic wireless network scenarios and employed the optimal trajectory for the DBSs to cooperatively navigate in the considered area to maximize coverage of the dynamic requests of the ground users. Chen *et al.* [32] studied the deployment of cache-enabled UAVs in a cloud radio access network and proposed a novel algorithm based on the machine learning framework of concept-based echo state networks (ESNs) to predict the users' content request distribution and their mobility pattern by leveraging prior knowledge of the limited information of users and the network. By using the prediction, the optimal locations of the UAVs and content to cache at UAVs are derived.

Different from the above works, we propose a laser charging enabled DBS assisted network to provide ubiquitous communications, which is extremely useful to support communications for disaster scenarios; the laser is used for charging the DBS, and the DBS is employed to provide communications for the ground users; the DBS placement, the power and bandwidth assignment, the laser charging rate and the energy consumption of the DBS are studied.

In this paper, the intelligent DBS placement is investigated in each time slot and a time slot is a fixed small time duration, during which the DBS hovers at a fixed location to serve user equipments (UEs). Meanwhile, the UE association, the power and bandwidth assignment need to be intelligently designed in order to maximize the total throughput of the network while the flight time of the DBS is extended. We formulate the joinpowEr and bandwidth assignment, LasEr Charing enAble DBS placemenT (TELECAST) problem, and jointly maximize the down link data rate and total flight time by optimizing the limited power and bandwidth allocation as well as the placement of the DBS.

The main contributions of this paper are delineated as follows:

- 1) We propose a laser charging enabled DBS framework where the laser is implemented for both communications and charging. A laser charging station is placed on the ground and it constantly transmits energy to a DBS while the DBS provides communications to the ground users.
- 2) We propose a charging model with laser charging from the perspective of the battery to estimate the flight time of the DBS.
- 3) We propose a recursive algorithm to solve the joint power and bandwidth allocation (JPB) problem iteratively and a counting placement algorithm to solve the DBS placement problem.

The rest of this article is organized as follows. The system model and the problem formulation is presented in Section II. Two heuristic algorithms are proposed in Section III. The algorithm performance evaluation is shown in Section IV. Section V presents the conclusion.

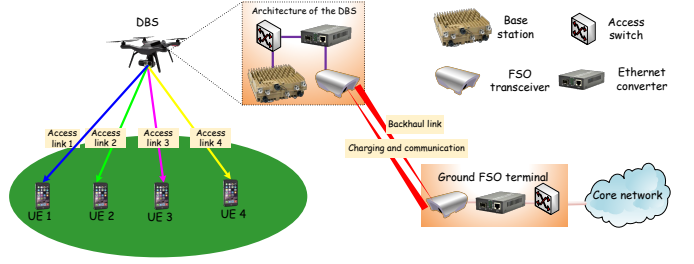


Fig. 1: A laser charging enabled DBS assisted wireless communications network

II. SYSTEM MODEL AND PROBLEM FORMULATION

We propose a laser charging enabled DBS assisted wireless communications network to serve the ground UEs in a disaster area or provide ubiquitous communications for temporary events, as expressed in Fig. 1. The wireless communications network consists of a DBS, a group of ground UEs and a laser charging station. We assume that each UE has a determined data rate requirement in every time slot and the power and bandwidth resource in the DBS is limited. The DBS flies at a fixed height and uses RF to provide services to the ground UEs. The charging station is equipped with a laser power source to provide both data and energy for the DBS to extend its service time. Another laser, mounted on the charging station, is used for backhaul communications. The height of the DBS and that of the charging station are high enough to provide LoS links. According to [28] [29], the data rate of an FSO channel can reach more than 100 Gbps for 1–1.5 km transmission, and the backhaul link has enough capacity to accommodate all UEs. Then, we only focus on the optimization of the resource assignment and placement of the DBS. Note that the DBS needs to reserve enough energy to return to the charging station. The ground UEs' positions are known and assumed to be of low mobility. The DBS may change its position in every time slot in order to harvest energy while maximizing the total data rate of all UEs.

A. Communications Model

The communications channel between the DBS and UEs at location i is assumed to be probabilistic line of sight (LoS). The probability of LoS can be written as [8]:

$$p^{los} = \frac{1}{1 + ae^{-b(\theta_i - a)}}, \quad (1)$$

where a and b are environmental parameters related to a specific area such as rural, urban and other terrain [16]. θ_i is the elevation angle between the DBS and UE_i , which can be expressed as $\theta_i = \arctan(l/\delta_i)$, where l is the height of the DBS and δ_i is the horizontal distance between the DBS and UE_i .

The LoS and non-LoS path loss between the DBS and UE_i can be written as:

$$\varphi_i^{los} = \xi^{los} + \tau^{los} \log_{10}(\sqrt{\delta_i^2 + l^2}) \quad (2)$$

$$\varphi_i^{Nlos} = \xi^{Nlos} + \tau^{Nlos} \log_{10}(\sqrt{\delta_i^2 + l^2}), \quad (3)$$

where ξ^{los} and ξ^{Nlos} are the path loss at the reference distance, and τ^{los} and τ^{Nlos} are the path exponent for LoS and non-LoS connection, respectively [17], [18]. Since we know the probability mass function of the LoS and non-LoS data rate, the average data rate of UE_i when communicating with the DBS in time slot n is expressed as:

$$\begin{aligned} R_i[n] = & b_i[n] \log_2 \left(1 + \frac{p_i[n] \varphi_i^{los}[n]}{N_0 b_i[n]} \right) p^{los} \\ & + b_i[n] \log_2 \left(1 + \frac{p_i[n] \varphi_i^{Nlos}[n]}{N_0 b_i[n]} \right) (1 - p^{los}), \end{aligned} \quad (4)$$

where p_i denotes the transmission power assigned to UE_i by the DBS; p_i remains the same over time slot n ; N_0 is the power spectral density of white Gaussian noise and assumed to be identical for all UEs; b_i is the bandwidth allocated to UE_i by the DBS.

B. Laser Power Model

We consider free space optical propagation between the DBS and the laser charging station. G_t denotes the charging station transmission gain and the transmitting power P_t . The power received at the DBS can be expressed as [6]:

$$P_r = P_t G_t G_r \tau_t \tau_e \tau_r P, \quad (5)$$

where τ_t and τ_r denote the optical efficiency at the transmitter and receiver, respectively; $\tau_e = 10^{-\alpha L/10}$ is the environmental attenuation parameter, where L is the distance between the DBS and the charging station and α is the environmental factor with α being 0.19 dB/km in clear weather, 6.9 dB/km when foggy and 28.9 dB/km in moderate fog. $P = (\lambda/4\pi L)^2$ is the free space path loss, where λ is the wavelength of the laser; $G_r = (\pi D/\lambda)^2$ is the DBS's receiver gain, where D is the receiver diameter; $G_t = 16/\Theta^2$ is the transmitter gain, where Θ is the divergence angle [7]. We can rewrite Eq. (6) as:

$$P_r = P_t (D/\Theta L)^2 \tau_t 10^{-\alpha L/10} \tau_r. \quad (6)$$

C. Charging Model

The DBS uses a lithium battery to provide energy. The amount of charge in the battery when fully charged is Q . Based on the Coulomb counting method, the battery state of charge is expressed as [19]:

$$S(t) = 1 - \frac{1}{Q} \int_0^t I(\zeta) d\zeta. \quad (7)$$

The remaining amount of charge in the battery can be expressed as [20]:

$$Q(t) = S(t)Q. \quad (8)$$

The remaining flight time of the DBS can be expressed as:

$$T(t) = \frac{Q(t)\eta_m\eta_e}{I^d}, \quad (9)$$

where I^d is the average working current of the DBS, η_m is the motor efficiency and η_e is the battery discharging efficiency.

The received laser energy is assumed to provide relatively stable voltage for the DBS. The amount of charge in the battery while charging equals to the initial amount of charge minus the amount of charge used by the DBS plus the amount of charge harvested from the laser. The remaining flight time of the DBS while charging can be expressed as:

$$T(t) = \frac{Q(t)\eta_m\eta_e}{I^d} + \frac{\frac{\eta_m\eta_e\eta_c}{V} \int_0^t P_r(\zeta) d\zeta}{I^d}. \quad (10)$$

The first part of the formula is the remaining usage time after the battery is discharged, and the second part is the extra flight time converted by the DBS after collecting the laser energy. Here, η_c is the converting efficiency of the charging circuit on the DBS. V is the working voltage of the DBS.

To simplify the problem, we define $\Gamma[n]$ as the remaining service time at the end of the n -th time slot, as expressed in Eq. (11):

$$\Gamma[n+1] = \Gamma[n] - \Gamma^{used}[n+1] + \Gamma^{charged}[n+1]. \quad (11)$$

Here, the reduced service time due to the DBS movement and hovering in the $n+1$ -th time slot can be expressed as:

$$\Gamma^{used}[n+1] = \tau_0 + \frac{E[n+1]}{I^d V}, \quad (12)$$

where τ_0 is the duration of a service period. $\frac{E[n+1]}{I^d V}$ is the reduced DBS service time due to the movement energy consumption in the $(n+1)$ -th time slot. The energy consumed by the DBS while moving from one location to another location in the $(n+1)$ -th time slot is defined as $E[n+1]$, which can be calculated by kinetic energy $E[n+1] = k\nu^2[n+1]$ [21]. Here, the energy parameter is $k = 0.5M$. M is the mass of the DBS.

The extended service time harvested from laser energy in the $(n+1)$ -th time slot can be expressed as:

$$\Gamma^{charged}[n+1] = \frac{\eta_m\eta_e\eta_c\tau_0}{I^d V} P_r[n+1]. \quad (13)$$

$\Gamma[0]$ can be obtained by calculating the average hovering time of the DBS without charging.

The ground UEs are assumed to be of low mobility so that the DBS will not change its location frequently. The movement time is negligible as compared to the service period. So, the remaining service time at the end of the $(n+1)$ -th service period equals to the remaining service time minus the service period and the reduced service time due to the movement of the DBS, plus the extended time converted from the laser energy in the $(n+1)$ -th service period.

D. Problem Formulation

In this paper, we aims to extend the DBS's flight time and maximize the total data rate. Here, $X[n]$ and $Y[n]$ are the location of the DBS at time slot n . p_i and b_i are the power

and bandwidth allocated to UE_i . $Z[n]$ is a boolean variable. If the DBS has enough battery energy to serve UE and return to the charging station at the n -th time slot, $Z[n] = 1$; otherwise, $Z[n] = 0$. Then, the summation of $Z[n]$ indicates the number of time slots that the DBS serves ground UEs. $\omega_i[n]$ is the UE association indicator and it is “1” if UE_i is served at time slot n . Therefore, the throughput of the network at time slot n can be expressed as $\sum_i \omega_i[n] R_i[n]$. The TELECAST problem can be formulated as a multi-objective optimization:

$$\begin{aligned}
\mathcal{P}_1 : \quad & \max_{X[n], Y[n], b_i[n], p_i[n], \omega_i[n], Z[n]} \sum_n Z[n] \\
& \max_{X[n], Y[n], b_i[n], p_i[n], \omega_i[n], Z[n]} \sum_n \sum_i \omega_i[n] R_i[n] \\
s.t. : \quad & C1 : \omega_i[n] \leq Z[n], \forall i \in \{1, 2, \dots, K\}, \forall n \in \{1, 2, \dots\} \\
& C2 : \sum_{i=1}^K \omega_i[n] b_i[n] \leq \beta, \forall n \in \{1, 2, \dots\} \\
& C3 : \sum_{i=1}^K \omega_i[n] p_i[n] \leq P^{th}, \forall n \in \{1, 2, \dots\} \\
& C4 : \Gamma[n] - \Gamma^{th} \geq (Z[n] - 1) \cdot f_0 \\
& C5 : \Gamma[n] - \Gamma^{th} < Z[n] \cdot f_0 \\
& C6 : 0 \leq X[n] \leq X_{max} \\
& C7 : 0 \leq Y[n] \leq Y_{max} \quad (14)
\end{aligned}$$

$C1$ is the battery constraint, which ensures the DBS to serve with enough power. $C2$ is the bandwidth capacity constraint, which imposes the bandwidth provisioned to UEs not to exceed the total bandwidth capacity of the DBS. $C3$ is the communications power capacity constraint, which imposes the total power assigned to UEs for communications not to exceed the maximum communications power of the DBS. $C4-C5$ are the DBS energy constraints, which impose the DBS to reserve enough energy to return to the charging station. Note that the received laser energy can only extend the flight time rather than allowing the DBS to fly forever. $C6-C7$ are the DBS placement constraints on the horizontal plane.

III. PROPOSED SOLUTION

The TELECAST problem is NP hard due to the bandwidth and power resource allocation. The resource allocation problem can be mapped into a two-dimensional knapsack problem. A UE can be mapped into an item, the required bandwidth and power consumption can be mapped into the weight and the volume, and the data rate can be mapped into the profit (value). The objective is to maximize the throughput of the network by optimizing the limited bandwidth and power allocation. To tackle the TELECAST problem, we divide the problem into two sub-problems and solve the two sub-problems iteratively. The first sub-problem is the bandwidth and communications transmission power allocation problem. The second is the DBS placement problem. First, the DBS is placed at a random location and assigns the bandwidth and power to every UE to achieve the maximum data rate. Then, the DBS flies to a location where it can harvest the largest amount of laser energy while maintaining the UE association.

TABLE I: Parameters

b_i	bandwidth of UE_i
p_i	communications power of UE_i
ω_i	UE association indicator
β	bandwidth capacity of the DBS
P^{th}	communications power capacity of the DBS
R_i	data rate of UE_i
Γ_0	initial flight time of the DBS
$\Gamma[n]$	remaining flight time of the DBS at the end of time slot n
Γ^{th}	time for the DBS to return to the charging station
$Z[n]$	DBS service indicator at time slot n
f_0	a large number, e.g., 10^9
I^d	working current of the DBS
V	working voltage of the DBS
$E[n]$	movement energy consumption of the DBS in time slot n
M	weight of the DBS
η_m	motor efficiency of the DBS
η_e	battery discharging efficiency
η_c	charging efficiency
$P_r[n]$	received laser power at time slot n
τ_0	duration of the time slot
K	number of UEs
$(X[n], Y[n])$	location of the DBS at time slot n
R	expected data rate of the RA-JPB algorithm
$B(j, R)$	the minimum bandwidth consumption for j UEs and R

A. The JPB Problem

For a given DBS placement, P_1 is simplified to:

$$\begin{aligned}
\mathcal{P}_2 : \quad & \max_{b_i[n], p_i[n], \omega_i[n]} \sum_n \sum_i \omega_i[n] R_i[n] \\
s.t. : \quad & C2 \text{ and } C3 \text{ in } \mathcal{P}_1 \quad (15)
\end{aligned}$$

The JPB problem focuses on maximizing the total throughput with limited communications and bandwidth resources. It is a two-dimensional knapsack problem, which is a well known NP hard problem. Every UE can either be served or ignored, and so the solution space is 2^K . The time complexity of the traditional backtracking or depth first search algorithm is $O(2^K)$, even leveraged with some sub-tree subtraction method.

To reduce the computational complexity, we first reduce the dimension of the problem by assigning the power of UE_i $p_i = \varsigma_i b_i$ [22]. ς_i is the power-spectral density of the i^{th} UE. Then, we convert the original problem to a minimum bandwidth consumption problem: there are K UEs, the data rate requirement of UE_i is R_i and the bandwidth requirement of UE_i is b_i . The total aggregated data rate is expected to be R . How to provision UEs such that the total data rate is at least R and $\sum b_i$ is the minimum is formulated as follows:

$$\begin{aligned}
\mathcal{P}_3 : \quad & \min_{\omega_i[n], b_i[n], R} \sum_n \sum_i \omega_i[n] b_i[n] \\
s.t. : \quad & C2 \text{ in } \mathcal{P}_1 \\
& C8 : \sum_{i=1}^K \omega_i[n] R_i[n] \geq R, \forall n \in \{1, 2, \dots\}, R \in [0, \sum R_i] \quad (16)
\end{aligned}$$

To solve the minimum bandwidth consumption problem, we define $B(j, R)$ as the smallest bandwidth consumption of UEs in providing the total data rate larger than or equal to R among $\{UE_1, UE_2, \dots, UE_j\}$. $B(j, R) = \min\{\sum_{i=1}^j \omega_i b_i | \sum_{i=1}^j \omega_i R_i \geq R\}$

$R, j \in \{1, 2, \dots, K\}$, $R \in [0, \sum_{i=1}^K R_i]$, $\omega_i = 0$ or 1 }. When $j = 0$, no UE is to be served. So, $B(0, R) = 0$ if the expected total data rate $R = 0$. If the expected total data rate $R > 0$, $B(0, R) = +\infty$ because there is no solution for the expected data rate to be larger than 0 if there is no UE to serve. The recursive relationship between UE_j and UE_{j+1} is defined as follows. If the data rate of UE_{j+1} already reaches the expected total data rate, there are two choices: we can either serve the previous j UEs or we only serve UE_{j+1} . Then, we chose the one that consumes less bandwidth. If the data rate of UE_{j+1} dose not meet the expected total data, there are two choices: we can serve the previous j UEs or $(j+1)$ UEs. Then, we chose the one that consumes less bandwidth. As a result, we get the recursive equation:

$$B(0, R) = \begin{cases} 0, & R = 0, \\ +\infty, & R > 0, \end{cases} \quad (17)$$

$$B(j+1, R) = \begin{cases} \min\{B(j, R), b_{j+1}\}, & R \leq R_{j+1}, \\ \min\{B(j, R), B\}, & R > R_{j+1}, \end{cases} \quad (18)$$

where $B = B(j, R - R_{j+1}) + b_{j+1}$.

Algorithm 1 is a recursive allocation algorithm, and it is designed based on the dynamic programming method to solve the JPB problem (RA-JPB), consisting of two parts. For the first part, the data rate of each UE R_i is scaled down to increase the running speed (*Steps 1-3*). Here, $R_i = \lceil \frac{K}{\epsilon A} R_i \rceil$, $(1 - \epsilon)$ is the approximation ratio. Since the dynamic programming can only solve the integer problem, we need to round the data rate of every user to an integer value in order to implement Algorithm 1. For the scalar A , the data rate of each UE R_i is not well scaled if A is set to a large value, and this will reduce the precision of Algorithm 1. The data rates of users would be very large after scaling and rounding if we set A to a small value, and this will incur a long time to find a solution for Algorithm 1. For example, R_i becomes 1 after scaling if A is set to infinity, and we are not able to find an appropriate solution. If $A = 0.005$, we can find a solution at the expense of long running time because R_i is 200 times larger. In this work, we set A equals to $\max\{R_1, R_2, \dots, R_K\}$, which is the lower bound of the optimal data rate we can achieve. Then, the solution is determined recursively. The second part includes two loops (*Steps 4-11*). The outer loop enumerates all the UEs and the inner loop enumerates all the expected data rates. The complexity of the outer loop is obviously $O(K)$ and the complexity of the inner loop is $O(KA)$. Then, the complexity of the RA-JPB algorithm is $O(KA)$. This algorithm maintains a table to record the bandwidth consumption for every UE and its achievable total data rate. Thus, the space complexity is also $O(K^2A)$.

Theorem 1. *The RA-JPB algorithm can yield a near-optimal solution of $(1 - \epsilon)R^{opt}$.*

Proof. Let S be the set of UEs that achieves the optimal total rate. Let R_i^* be the data rate after scaling and rounding. Let S^* be the set of UEs that achieves the optimal total rate after scaling and rounding. We have $\sum_{i \in S^*} R_i^* \geq \sum_{i \in S} R_i^*$. Moreover, $\frac{K}{\epsilon A} R_i \leq R_i^* \leq \frac{K}{\epsilon A} R_i + 1$. Hence, we can derive that $R^{opt} = \sum_{i \in S} R_i \leq \frac{\epsilon A}{K} \sum_{i \in S} R_i^* \leq \frac{\epsilon A}{K} \sum_{i \in S^*} (\frac{K}{\epsilon A} R_i + 1) = (1 + \frac{1}{\epsilon A}) \sum_{i \in S^*} R_i^* = (1 + \frac{1}{\epsilon A}) R^{opt}$.

Algorithm 1: Recursive Allocation for JPB (RA-JPB)

Input: $K, \epsilon, \beta, P^{th}, UE, b_i, p_i$;
Output: ω_i, r^*, b_i, p_i ;

- 1 $A = \max R_i$;
- 2 **for** $i \in K$ **do**
- 3 $R'_i = \lceil \frac{K}{\epsilon A} R_i \rceil$;
- 4 **for** $j \in K$ **do**
- 5 **while** $R \leq K \max R_i$ **do**
- 6 | **if** $R \leq R_{j+1}$ **then**
- 7 | | $B(j+1, R) = \min\{B(j, R), b_{j+1}\}$;
- 8 | **if** $R > R_{j+1}$ **then**
- 9 | | $B(j+1, R) = \min\{B(j, R), B(j, R - R_{j+1}) + b_{j+1}\}$;
- 10 | | $R = R + 1$;
- 11 | | $j = j + 1$;
- 12 **return** $B^* = B(K, R)$ and $r^* = R$;

1) $\leq \sum_{i \in S^*} R_i + \frac{\epsilon A}{K} K$. Since $A \leq R^{opt}$, we can derive that $(1 - \epsilon)R^{opt} \leq \sum_{i \in S^*} R_i$. \square

Theorem 2. *The minimum bandwidth consumption problem is an NP complete problem.*

Proof. Note that the minimum bandwidth consumption problem is a decision-making problem: given a set K with k items with size b_1, b_2, \dots, b_k . The values of the k items are R_1, R_2, \dots, R_k . The bandwidth capacity is β ; R is the expected value. Is there a subset $S \in K$ such that $\sum_{i \in S} b_i \leq \beta$ and $\sum_{i \in S} R_i \geq R$?

First, we prove that the decision problem can be verified in polynomial time. For a given set S , to determine whether it meets the conditions of $\sum_{i \in S} b_i \leq \beta$ and $\sum_{i \in S} R_i \geq R$, we need $2 \cdot (|S| - 1)$ operations, where $|S|$ is the number of items in the set S . The time complexity is $O(2 \cdot (|S| - 1))$, which is polynomial.

Second, we show that there is a polynomial reduction from the partition problem to the minimum bandwidth consumption problem. Suppose we are given positive numbers a_1, a_2, \dots, a_n for the partition problem. The task is to decide whether these numbers can be partitioned into two sets S and T such that the sum of the numbers in S equals the sum of the numbers in T . Consider a knapsack problem: $b_i = a_i, R_i = a_i$ for $i \in \{1, 2, \dots, n\}$, $\beta = R = \frac{1}{2} \sum_{i=1}^n a_i$. The process to convert the partition problem to the knapsack problem is clearly polynomial. If X is a TURE instance for the partition problem, there exists S and T such that $\sum_{i \in S} a_i = \sum_{i \in T} a_i = \frac{1}{2} \sum_{i=1}^n a_i$. Let the knapsack contain the items in S and $\sum_{i \in S} b_i = \sum_{i \in S} a_i = \beta$ and $\sum_{i \in S} R_i = \sum_{i \in S} a_i = R$. Therefore, X' is a TURE instance for the knapsack decision problem. If X' is a TURE instance for the knapsack decision problem, with the chosen set S , let $T = \{1, 2, \dots, n\} - S$. We have $\sum_{i \in S} b_i = \sum_{i \in S} a_i \leq \beta = \frac{1}{2} \sum_{i=1}^n a_i$ and $\sum_{i \in S} b_i = \sum_{i \in S} a_i \geq R = \frac{1}{2} \sum_{i=1}^n a_i$. This implies that $\sum_{i \in S} a_i = \sum_{i \in T} a_i$. Therefore, S and T are the desired partitions, and X is a TURE instance for the

partition problem. This establishes the NP completeness of the minimum bandwidth consumption problem. \square

Theorem 3. *The minimum bandwidth consumption problem exhibits the optimal substructure.*

Proof. An optimization problem has the optimal substructure if the optimal solution can be constructed from optimal solutions of its subproblems. Let $\{\omega_1, \omega_2, \dots, \omega_k\}$ be the solution for the minimum bandwidth consumption problem with the bandwidth consumption of $B(k, R^{opt})$. For each UE, it has two different statuses: served or not served. Without loss of generality, we analyze the provisioning process of one UE (e.g., the j -th UE) to prove the optimal substructure and the rest UEs (excluding the j -th UE) are served. For the j -th UE, it has two different serving statuses: 1) It is served, $\omega_j = 1$, implying that the best solution is $\{\omega_1, \omega_2, \dots, \omega_j, \dots, \omega_k\} = \{1, 1, \dots, 1, \dots, 1\}$ for the minimum bandwidth consumption problem and the bandwidth consumption is $B(k-1, R^{opt} - R_j) + b_j$; 2) It is not served, $\omega_j = 0$, implying that the best solution is $\{\omega_1, \omega_2, \dots, \omega_{j-1}, \omega_j, \omega_{j+1}, \dots, \omega_k\} = \{1, 1, \dots, 1, 0, 1, \dots, 1\}$ for the minimum bandwidth consumption problem and the bandwidth consumption is $B(k-1, R^{opt})$. We prove this theorem by contradiction.

Proof of case 1: $\omega_j = 1$. We assume $B(k-1, R^{opt} - R_j) + b_j$ is not the smallest bandwidth consumption, implying that $\{\omega_1, \omega_2, \dots, \omega_{j-1}, \omega_j, \omega_{j+1}, \dots, \omega_k\} = \{1, 1, \dots, 1, 0, 1, \dots, 1\}$, $B(k-1, R^{opt} - R_j) + b_j > B(k-1, R^{opt})$. Then, we have $B(k, R^{opt}) = B(k-1, R^{opt} - R_j) + b_j > B(k-1, R^{opt})$, which contradicts $B(k, R^{opt}) \leq B(k-1, R^{opt})$. Here, $B(k, R^{opt})$ and $B(k-1, R^{opt})$ are the least required bandwidth for serving k UEs and $(k-1)$ UEs to achieve R^{opt} ; $B(k, R^{opt}) \leq B(k-1, R^{opt})$ because the former has more flexibility to choose UEs with less required bandwidth among k UEs. Thus, we have $\omega_j = 1$, $B(k-1, R^{opt} - R_j) + b_j$ is the smallest bandwidth consumption, and the optimal solution is $\{\omega_1, \omega_2, \dots, \omega_j, \dots, \omega_k\} = \{1, 1, \dots, 1, \dots, 1\}$.

Proof of case 2: $\omega_j = 0$. We assume $B(k-1, R^{opt})$ is the smallest bandwidth consumption, implying that $\{\omega_1, \omega_2, \dots, \omega_j, \dots, \omega_k\} = \{1, 1, \dots, 1, \dots, 1\}$, $B(k, R^{opt}) = B(k-1, R^{opt} - R_j) + b_j$ and $B(k-1, R^{opt}) < B(k-1, R^{opt} - R_j) + b_j$. Then, we have $B(k, R^{opt}) < B(k-1, R^{opt}) < B(k-1, R^{opt} - R_j) + b_j$, which contradicts $B(k, R^{opt}) = B(k-1, R^{opt} - R_j) + b_j$. Thus, we have $\omega_j = 0$, $B(k-1, R^{opt})$ is not the smallest bandwidth consumption, and the optimal solution is $\{\omega_1, \omega_2, \dots, \omega_{j-1}, \omega_j, \omega_{j+1}, \dots, \omega_k\} = \{1, 1, \dots, 1, 0, 1, \dots, 1\}$. Based on the above proof, we conclude that the minimum bandwidth consumption problem of the JPB problem exhibits optimal substructure. \square

B. DBS Placement Problem

For a given horizontal plane and UE scheduling, the DBS placement problem can be simplified as:

$$\mathcal{P}_4 : \max_{X[n], Y[n], \omega_i[n], b_i[n], p_i[n]} \sum_n Z[n]$$

s.t. :

$$C1 : \sum_{i=1}^K \omega_i[n] b_i[n] \leq \beta, \forall n \in \{1, 2, \dots\}$$

$$\begin{aligned} C2 : \sum_{i=1}^K \omega_i[n] p_i[n] &\leq P^{th}, \forall n \in \{1, 2, \dots\} \\ C3 : \Gamma[n] - \Gamma^{th} &\geq (Z[n] - 1) \cdot f_0 \\ C4 : \Gamma[n] - \Gamma^{th} &< Z[n] \cdot f_0 \\ C5 : 0 \leq X[n] &\leq X_{max} \\ C6 : 0 \leq Y[n] &\leq Y_{max} \end{aligned} \quad (19)$$

Algorithm 2: Counting Placement (CP)

```

Input:  $\omega_i, R_i, X_{max}, Y_{max}, \Gamma[n], \Gamma^{th}, r^*$ ;
Output:  $X^*, Y^*, Z_n$ ;
1 for  $X \in X_{max}$  and  $Y \in Y_{max}$  do
2   calculate  $b_i$  and  $p_i$  according to  $\omega_i$  and  $R_m$ ;
3 for  $m \leq M$  do
4   if  $R_m > B_{max}$  then
5      $B_{max} = R_m$ ;
6   if  $R_m < B_{min}$  then
7      $B_{min} = R_m$ ;
8    $R_a = B_{max} - B_{min} + 1$ ;
9 for  $m \leq M$  do
10    $index = \lceil R_m - B_{min} \rceil$ ;
11    $C_o(index) = C_o(index) + 1$ ;
12  $index = 1$ ;
13 for  $m \leq R_a$  do
14   while  $C_o(m) \geq 1$  do
15      $R(index) = m + \min$ ;
16      $index = index + 1$ ;
17      $C_o(m) = C_o(m) - 1$ ;
18  $m = M$ ;
19 for  $m > \frac{3}{4}M$  do
20   if  $r^* \leq R(m)$  and  $\Gamma \leq \Gamma^*$  then
21     if  $\sum_{i=1}^K \omega_i[n] b_i[n] \leq \beta$  and
22        $\sum_{i=1}^K \omega_i[n] p_i[n] \leq P^{th}$  then
23        $r^* = R(m)$ ;
24        $\max \Gamma = \Gamma^*$ ;
25        $m = m - 1$ ;
26  $(X^*, Y^*) = \arg \max \Gamma(X_n, Y_n)$ ;
27 if  $\Gamma[n] - \Gamma^{th} > 0$  then
28    $Z[n] = 1$ ;
29 else
30    $Z[n] = 0$ ;
31    $\omega_i = 0 \forall i \in K$ ;

```

To determine the DBS's location, we first divide the searching plane into several blocks and calculate the total data rate at each block. Second, we sort these blocks in ascending order according to the total data rate. To decrease the complexity, we compare R^{opt} and data rate in the sequence in reverse order. If there is a location where the DBS can harvest more energy while maintaining the data rate R^{opt} , the DBS will move to that location. $Z[n] = 0$ indicates that the DBS does not have enough energy to fly back to the station even with the laser

charging at the end of time slot n . When $Z[n] = 0$, ω_i is set to 0 for all UEs, i.e., the DBS does not have enough energy and will not serve any UE.

Algorithm 2 is based on the Counting Sort algorithm. In Algorithm 2, Counting Placement (CP), the plane is divided into M blocks and the throughput of the m -th block R_m is calculated (*Steps 1-2*). B_{max} and B_{min} are two blocks that have the maximum and minimum throughput among all blocks, respectively (*Steps 3-8*). R_a is the variance between the maximum and minimum throughput. C_o is an auxiliary array. Here, index is used to count how many blocks can provision a data rate of R_m . The number of blocks with throughput R_m is stored in C_o (*Steps 9-11*). The blocks are sorted according to the throughput (*Steps 13-17*). A location that can maintain the throughput of the network is determined from *Steps 18-25* of Algorithm 1. The energy status of the DBS is checked (*Steps 26-30*). The complexity of the counting placement (CP) algorithm depends on the number of blocks. The complexity of calculating the data rate at each sub-plane is $O(MK^2A)$. The complexity of sorting sub-planes is $O(M + R_a)$. The complexity of obtaining the energy of each candidate sub-plane is $O(\frac{1}{4}M)$. As a result, the complexity of the CP algorithm is $O(MK^2A + M + R_a)$.

IV. PERFORMANCE EVALUATION

We use MATLAB to conduct the simulation. The DBS is deployed to respond to an emergency. So, for every simulation, 60 UEs are randomly distributed in a $300 \times 300 \text{ m}^2$ area. One DBS is deployed as a base station to serve the UEs. To illustrate that the laser enables UAV to serve users far away, the laser charging station is placed at $(0, 0)$ point of the Cartesian coordinate and the UEs are randomly distributed at $x \in [100, 400]$ and $y \in [100, 400]$. To simplify the simulation, the DBS is initially placed in the middle of the UEs ($\frac{\sum_{i=1}^K x_i}{K}, \frac{\sum_{i=1}^K y_i}{K}$) and gradually change their locations in every time slot. We use the quadcopter UAV DJI MATRICE 100 specifications to run the simulations. The working voltage is 23V, the working current is 5A and 4W is assigned for communications. The output of the charging station is 200W [23]. The original flight time of the DBS without charging is 30 minutes. Considering low mobility, we divide the original flight time into 10 slots; each slot is 2 minutes. The other parameters are summarized in Table 2.

TABLE II: Simulation Parameters

(a, b)	$(9.1, 0.16)$ [24]	(ξ^{los}, ξ^{Nlos})	$(1, 20)$
$(\tau^{los}, \tau^{Nlos})$	$(20, 20)$	N_0	-174 dbm/Hz
β	10MHz	v	18m/s
l	25m	P^{th}	4W
P_t	200W	D	1.5
θ	0.01	α	6.9db/km [25]
I^d	5A	V	23V
M	3.6kg [3]	η_m	0.85
η_e	0.95	η_c	0.4
τ_t	0.7	τ_r	0.5
Γ_0	30min	τ_0	2min
K	60	(X_{max}, Y_{max})	$(400, 400)$ m

A. Algorithm Comparison

In this section, we compare our proposed algorithm with the fixed placement DBS algorithm, the Lagrange resource allocation algorithm, the greedy resource allocation and UE association algorithm, and the fixed placement with random UE association algorithm. We have also compared the proposed algorithm for different UE distributions and laser transmission power.

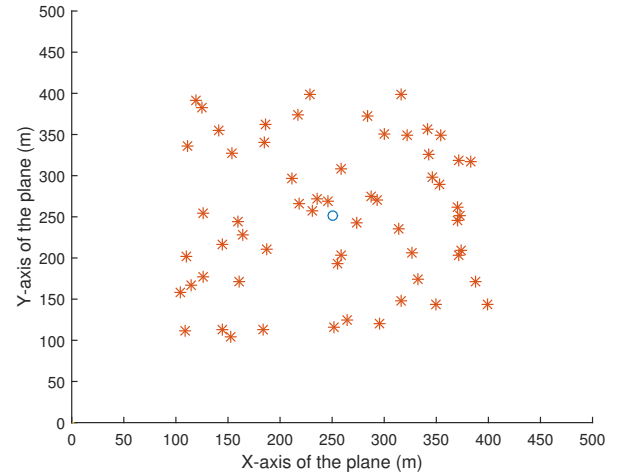


Fig. 2: Distribution 1 of UEs

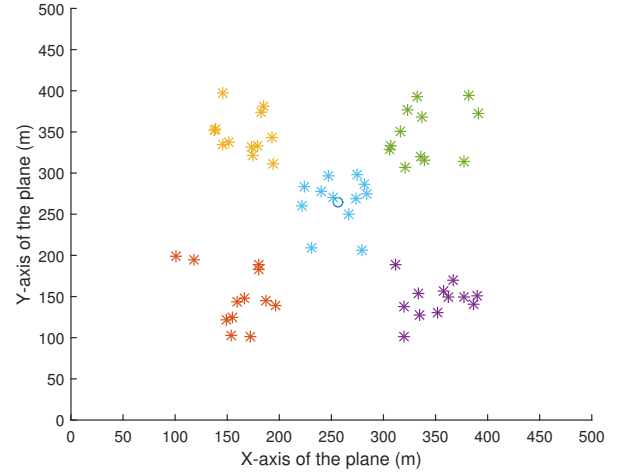


Fig. 3: Distribution 2 of UEs

Fig. 2 and Fig. 3 show two distributions of UEs in the horizontal plane. In Fig. 2, UEs are uniformly distributed in the plane. In Fig. 3, UEs are sparsely distributed and form different clusters in the plane.

Fig. 4 shows the laser energy harvested by the DBS. The distribution of UEs is illustrated in Fig. 2. As the distribution of UEs becomes denser, the DBS is able to find the best service location easier. The movement of the DBS is relatively small in every time slot, and, as a result, the yellow curve in Fig. 5 shows that the received energy grows slowly and steadily. With the sparse distribution as shown in Fig. 3, the UEs are form different clusters, and the DBS will fly between different clusters to find the best service locations. The received energy

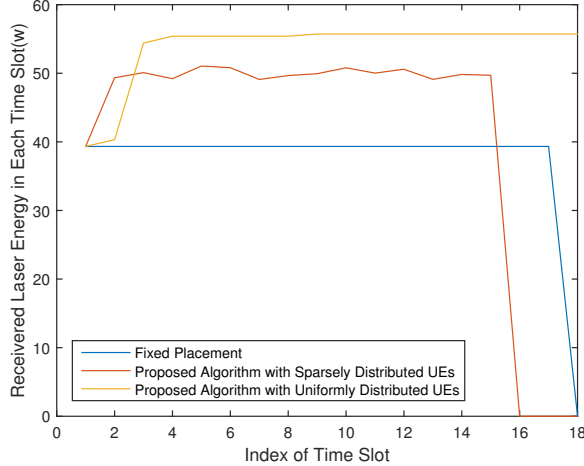


Fig. 4: Received energy

fluctuates in every time slot. If the DBS does not have enough energy to fly back to the charging station at the beginning of the next time slot, it will fly back to the charging station and stop serving UEs. So, at time slot 16 and 18, the received energy becomes zero for the "sparsely distributed UEs" and the "Fixed Placement", respectively.

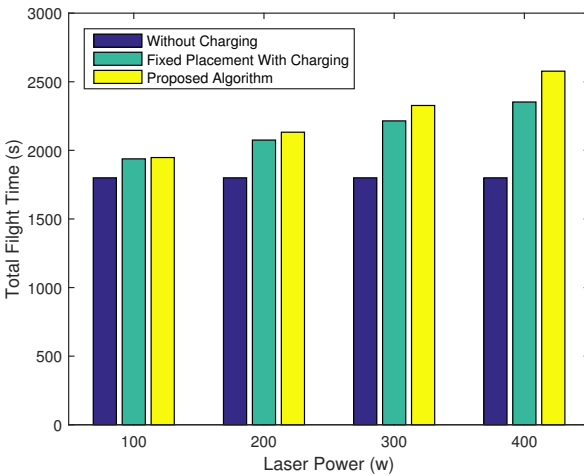


Fig. 5: Total flight time with different laser charging power

Fig. 5 demonstrates how the total flight time increases with different laser transmission power and DBS placement. The distribution of UEs is illustrated by Fig. 2. The blue bars are the original flight time of the DBS without laser charging. The green bars are the total flight time when the DBS is fixed in the middle of the UEs. The yellow bars are the total flight time by the proposed algorithm. From the simulation results, the total flight time increases as the laser power grows and our proposed algorithm is better than the fixed placement algorithm. When there are 60 users and the laser power is set to 200 W, the total flight time is extended 20% as compared with the flight time without charging and 3.5% of the total flight time is extended as compared with fixed placement algorithm. When the laser power is set to 400 W, our proposed algorithm can extend 43% of the total flight time as compared with the flight time without charging and 14% of the total flight time

is extended as compared with the fixed placement algorithm. Our proposed algorithm is superior to the fixed placement algorithm because our proposed algorithm enables the DBS to fly closer to the charging station. When the DBS finds the best placement, more energy can be harvested as compared with the fixed placement algorithm.

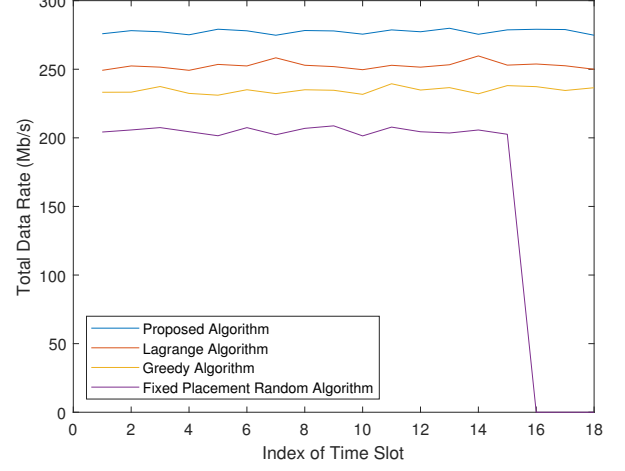


Fig. 6: Total data rate

Fig. 6 shows how the total data rate changes in 18 time slots as compared with three baseline algorithms for 60 UEs. For the Lagrange algorithm, the resource allocation follows that reported in [33]. To allocate the resource fairly, we assign the bandwidth equally and calculate the power assignment according to the data rate requirement. Then, the Lagrange function is constructed by combining the objective function, the Lagrange multiplier and the power capacity constraint. Eventually, we maximize the throughput by maximizing the Lagrange function. For the greedy algorithm, the DBS always serves the UE that requires the highest data rate per unit power. The bandwidth is equally assigned to UEs and the transmission power is calculated according to the requirement of each UE. Then, UEs are sorted in ascending order by the required data rate over the required transmission power. The DBS continues to serve the UEs until the bandwidth or power resource is exhausted. Our proposed algorithm is better than the greedy algorithm because the recursive algorithm finds the best scheduling to maximize the total throughput. However, the greedy algorithm selects UEs with better power efficiency. The random algorithm fixes the DBS in the middle of the UEs and then randomly picks UEs to serve until either the bandwidth or communications power is exhausted. Extensive simulation results have been demonstrated that our proposed algorithm is superior to the three baseline algorithms and the improvement of the total data rate of the proposed algorithm is up to 15% and 6% as compared to the greedy algorithm and the Lagrange algorithm, respectively.

B. Parametric Study

In this section, we conduct a parametric study involved in the system model by evaluating the effects of various parameters on the performance metrics, including the receiver

efficiency τ_r , converting efficiency of the charging circuit η_c and the number of UEs. Fig. 7 shows the total flight time with

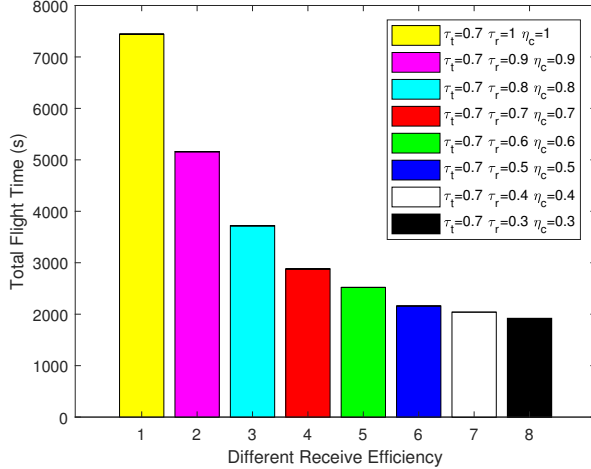


Fig. 7: Total flight time with different receiver efficiency

different receiver efficiencies for the UE distribution illustrated in Fig. 1. In Fig. 7, the y-axis represents the total DBS flight time and the x-axis corresponds to eight receiver efficiency scenarios. Here, τ_r is the receiver efficiency and η_c is the converting efficiency of the charging circuit. The results show that as the receiver efficiency decreases, the total flight time decreases accordingly. The flight time illustrated by the last column (black) is the same as the flight time without charging. Here, we concluded that when the laser power is 200w and the laser transmission efficiency is 0.7, the receiver efficiency and converting efficiency should be both at least 0.4 to extend the flight time with our proposed algorithm.

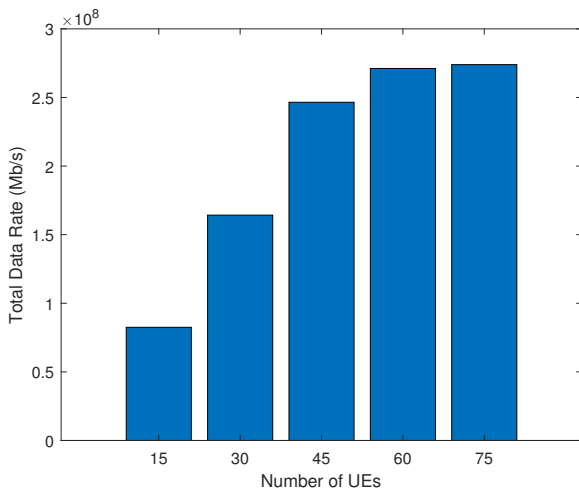


Fig. 8: Total UE data rate

Fig. 8 shows the total data rate versus the number of UEs. The total data rate increases as the number of UEs increases. The total data rate plateaus after 60 UEs because the power and bandwidth in the DBS are exhausted.

V. CONCLUSION

In this paper, we have formulated the joint power and bandwidth assignment, laser charging enabled DBS placement (TELECAST) problem in which the DBS is deployed to provide downlink communications to UEs on the ground and a laser is employed to charge the DBS in the air as well as provide backhaul link for the DBS. Our objective is to jointly maximize the total downlink data rate and flight time. The problem is decomposed into two sub-problems: joint power and bandwidth allocation problem and the DBS placement problem. Then, we have proposed a recursive algorithm to solve the JPB problem to maximize the total data rate with limited bandwidth and communications power. We have developed a method to estimate the flight time of the DBS and extend the flying time by implementing the RA-JPB and CP algorithms. The results show that the flight time can be extended by as much as 20% when the laser power is 200w and the flight time can be extended by more than 40% when laser is 400w. As compared to the fixed place algorithm, our algorithm can improve the DBS service time by 14% when laser power is 400w. In this paper, we have proposed to utilize DBS to provide downlink communications to UEs on the ground and a laser to charge the DBS in the air as well as provide backhaul link communications for the DBS. We have demonstrated the viability of our proposed concept by extensive simulations. In practice, weather conditions such as windy or sunny days, the payload weight, the air resistance, and other parameters in the real world will affect the DBS flight time. For the future work, we will investigate how to provide service to UEs in the DBS-aided network with multi-UAVs and a more accurate battery and charging model; we will study how the FSO link impacts the communications over a long distance and under large UE demands.

REFERENCES

- [1] L. Zhang and N. Ansari, "A Framework for 5G Networks with In-band Full-duplex Enabled Drone-mounted Base-stations," *IEEE Trans. Wireless Commun.*, vol. 26, no.5, pp. 121-127, Oct. 2019.
- [2] <https://baofengtech.com/usermanual/X-Series-User-Guide.pdf>.
- [3] <https://www.dji.com/matrice600-pro>.
- [4] "Communications Status Report for Areas Impacted by Hurricane Maria," *Federal Communications Commission*, Jan. 2018. <https://docs.fcc.gov/public/attachments/DOC-348974A1.pdf>.
- [5] <https://arstechnica.com/information-technology/2017/11/att-drone-brings-lte-access-to-hurricane-damaged-puerto-rico/>.
- [6] A. Majumdar, "Free-space laser communication performance in the atmospheric channel," *J Optic Comm Rep* 2, 345-396 (2005).
- [7] N. Ansari, Q. Fan, X. Sun, and L. Zhang, "SoarNet," *IEEE Trans. Wireless Commun.*, vol. 26, no. 6, pp. 37-43, Dec. 2019.
- [8] A. Al-Hourani, S. Kandepan, and S. Lardner, "Optimal LAP altitude for maximum coverage," *IEEE Wireless Commun. Lett.*, vol. 3, no. 6, pp. 569-572, Dec. 2014.
- [9] J. Wang *et al.*, "Machine Learning Based Rapid 3D Channel Modeling for UAV Communication Networks," *2019 16th IEEE Annual Consumer Communications & Networking Conference (CCNC)*, Jan. 2019.
- [10] L. Zhang and N. Ansari, "Approximate Algorithms for 3-D Placement of IBFD Enabled Drone-mounted Base-Station," *IEEE Trans. Veh. Technol.*, vol. 68, no. 8, pp. 7715-7722, Jun. 2019.
- [11] T. M. Mostafa, A. Muhamar and R. Hattori, "Wireless battery charging system for drones via capacitive power transfer," *2017 IEEE PELS Workshop on Emerging Technologies: Wireless Power Transfer (WoW)*, Chongqing, 2017, pp. 1-6.
- [12] Q. Wu, Y. Zeng and R. Zhang, "Joint Trajectory and Communication Design for UAV-Enabled Multiple Access," *IEEE Glob. Commun. Conf.*, Singapore, 2017, pp. 1-6.

- [13] J. Ouyang, Y. Che, J. Xu and K. Wu, "Throughput Maximization for Laser-Powered UAV Wireless Communication Systems," in *Proc. of IEEE ICC*, Kansas City, MO, 2018, pp. 1-6.
- [14] M. Jiang, Y. Li, Q. Zhang and J. Qin, "Joint Position and Time Allocation Optimization of UAV Enabled Time Allocation Optimization Networks," *IEEE Trans. Commun.*, vol. 67, no. 5, pp. 3806-3816, May 2019.
- [15] Y. Sun, D. Xu, D. W. K. Ng, L. Dai and R. Schober, "Optimal 3D-Trajectory Design and Resource Allocation for Solar-Powered UAV Communication Systems," *IEEE Trans. Commun.*, vol. 67, no. 6, pp. 4281-4298, Jun. 2019.
- [16] M. Alzenad, A. El-Keyi and H. Yanikomeroglu, "3-D Placement of an Unmanned Aerial Vehicle Base Station for Maximum Coverage of Users With Different QoS Requirements," *IEEE Wireless Commun. Lett.*, vol. 7, no. 1, pp. 38-41, Feb. 2018.
- [17] Q. Fan and N. Ansari, "Towards Traffic Load Balancing in Drone-Assisted Communications for IoT," *IEEE Internet Things J.*, vol. 6, no. 2, pp. 3633-3640, Apr. 2019.
- [18] 3GPP TR 36.828 version 11.0.0, release 11, 3GPP Tech. Rep., 2012. URL <http://www.qtc.jp/3GPP/Specs/36828-b00.pdf>.
- [19] J. Chiasson and B. Vairamohan, "Estimating the state of charge of a battery," *IEEE Trans. Control Syst. Technol.*, vol. 13, no. 3, pp. 465-470, May 2005.
- [20] W. Zhang, L. Wang, and Li. Wang, "An improved adaptive estimator for state-of-charge estimation of lithium-ion batteries," *Journal of Power Sources*, vol.402, pp.422-433, Oct. 2018.
- [21] Y. Qian *et al.*, "User Association and Path Planning for UAV-Aided Mobile Edge Computing With Energy Restriction," *IEEE Wireless Commun. Lett.*, vol. 8, no. 5, pp. 1312-1315, Oct. 2019.
- [22] T. Han and N. Ansari, "Enabling Mobile Traffic Offloading via Energy Spectrum Trading," *IEEE Trans. Wireless Commun.*, vol. 13, no. 6, pp. 3317-3328, Jun. 2014.
- [23] U.S. Naval Research Laboratory <https://www.nrl.navy.mil/news/releases/researchers-transmit-energy-laser-power-beaming-demonstration>.
- [24] L. Zhang, Q. Fan, and N. Ansari "3-D Drone-Base-Station Placement With In-Band Full-Duplex Communications," *IEEE Commun. Lett.*, vol. 22, no. 9, Sept. 2018.
- [25] F. Levander and P. Sakari, "Design and Analysis of an All-optical Free-space Communication Link," Dissertation, Institutionen för teknik och naturvetenskap, 2002.
- [26] T. Qiao, "Drone Trajectory Optimization using Genetic Algorithm with Prioritized Base Stations," *IEEE 25th International Workshop on Computer Aided Modeling and Design of Communication Links and Networks*, pp. 1-6, 2020.
- [27] X. Sun, N. Ansari and R. Fierro, "Jointly Optimized 3D Drone Mounted Base Station Deployment and User Association in Drone Assisted Mobile Access Networks," *IEEE Trans. Veh. Technol.*, vol. 69, no. 2, pp. 2195-2203, Feb. 2020.
- [28] N. Cvijetic, D. Qian, J. Yu, Y. Huang and T. Wang, "100 Gb/s per-channel free-space optical transmission with coherent detection and MIMO processing," *35th European Conference on Optical Communication*, Vienna, 2009, pp. 1-2.
- [29] X. Liu, *et al.*, "128 gbit/s free-space laser transmission performance 80 in a simulated atmosphere channel with adjusted turbulence," *IEEE Photonics Journal*, vol. 10, no. 2, pp. 1-10, Apr. 2018.
- [30] H. Zhang, *et al.*, "Nature-Inspired Self-Organization, Control, and Optimization in Heterogeneous Wireless Networks," *IEEE Trans. Mobile Comput.*, vol. 11, no. 7, pp. 1207-1222, Jul. 2012.
- [31] M. Chen, *et al.*, "Caching in the Sky: Proactive Deployment of Cache-Enabled Unmanned Aerial Vehicles for Optimized Quality-of-Experience," *IEEE Journal on Selected Areas in Communications*, vol. 35, no. 5, pp. 1046-1061, May 2017.
- [32] Y. Hu, *et al.*, "Distributed Multi-agent Meta Learning for Trajectory Design in Wireless Drone Networks," *IEEE Journal on Selected Areas in Communications*, doi: 10.1109/JSAC.2021.3088689.
- [33] Marco Caserta, *et al.*, "The robust multiple-choice multidimensional knapsack problem," *Omega*, vol. 86, no. 5, pp. 16-27, 2019, ISSN 0305-0483.
- [34] T. J. Nugent and J. T. Kare, "Laser power for UAVs," *Laser Motive White Paper C Power Beaming for UAVs*, 2010.
- [35] M. C. Achtelik, *et al.*, "Design of a flexible high performance quadcopter platform breaking the MAV endurance record with laser power beaming," *IEEE/RSJ International Conference on Intelligent Robots and Systems*, pp. 5166-5172, Sept. 2011.



Weiqi Liu [S'20] (wl296@njit.edu) received his M.S. degree in Electrical Engineering from the New Jersey Institute of Technology (NJIT) in 2019. He is currently pursuing a Ph.D. in Electrical Engineering at NJIT. His research interests include UAV communications, wireless communications, mobile edge computing, and Internet of Things.



Liang Zhang [S'15 M'20] (lz284@njit.edu) received Ph.D. in Electrical Engineering from New Jersey Institute of Technology (NJIT) in 2020, M.S. from University of Science and Technology of China (USTC) in 2014, and B.S. from Huazhong University of Science and Technology (HUST) in 2006. He is the recipient of the Hashimoto Prize for the best doctoral dissertation in 2020. He also received a Travel Grant Award from IEEE GLOBECOM in 2016, the Best Paper Award from IEEE ICNC in 2014, and the National Scholarship of Graduate Students in China in 2013. His research interests include UAV communications, wireless communications, mobile edge computing, Internet of Things, and datacenter networks.



Nirwan Ansari [S'78-M'83-SM'94-F'09] (nirwan.ansari@njit.edu), Distinguished Professor of Electrical and Computer Engineering at the New Jersey Institute of Technology (NJIT), received his Ph.D. from Purdue University, MSEE from the University of Michigan, and BSEE (summa cum laude with a perfect GPA) from NJIT. He is also a Fellow of National Academy of Inventors.

He authored *Green Mobile Networks: A Networking Perspective* (Wiley-IEEE, 2017) with T. Han, and co-authored two other books. He has also (co-)authored more than 600 technical publications. He has guest-edited a number of special issues covering various emerging topics in communications and networking. He has served on the editorial/advisory board of over ten journals including as Associate Editor-in-Chief of IEEE Wireless Communications Magazine. His current research focuses on green communications and networking, cloud computing, drone-assisted networking, and various aspects of broadband networks.

He was elected to serve in the IEEE Communications Society (ComSoc) Board of Governors as a member-at-large, has chaired some ComSoc technical and steering committees, is current Director of ComSoc Educational Services Board, has been serving in many committees such as the IEEE Fellow Committee, and has been actively organizing numerous IEEE International Conferences/Symposia/Workshops. He is frequently invited to deliver keynote addresses, distinguished lectures, tutorials, and invited talks. Some of his recognitions include several excellence in teaching awards, a few best paper awards, NCE Excellence in Research Award, several ComSoc TC technical recognition awards, NJ Inventors Hall of Fame Inventor of the Year Award, Thomas Alva Edison Patent Award, Purdue University Outstanding Electrical and Computer Engineering Award, NCE 100 Medal, NJIT Excellence in Research Prize and Medal, and designation as a COMSOC Distinguished Lecturer. He has also been granted more than 40 U.S. patents.